Photometric analysis of asteroid 7 (Iris) and other minor planets with the HATNet survey

Benjamin A. Cook

Princeton University Department of Astrophysical Sciences

Peyton Hall, Princeton, NJ 08544, USA

bacook@princeton.edu

April 28, 2013

ABSTRACT

The *HATNet* survey, which uses small telescopes with carefully calibrated CCD detectors to identify exoplanets using the transit method, is well suited to generate accurate *light curves* of *minor planets* (also known as *asteroids*) which coincidentally are captured in its images. Through collaboration with the HATNet team, we develop a procedure to locate and perform photometry on minor planets from cataloged HATNet frames. With many observations of the same minor planet timed closely together, we are able to derive a light curve for the object and calculate a rotation period. We perform this analysis for asteroid 7 (Iris) and obtain a period of 7.141 ± .012 hours, in agreement with the literature. We additionally discuss how an improved catalog of minor planet orbital elements, including past element values, can encourage the use of data from similar survey projects to generate asteroid light curves.

1. Introduction

1.1. What is a light curve and why is it curved?

The practice of light curve photometry is, generally speaking, simply the study of the brightness of an astronomical object as a function of time. With the advent of electronic CCD (charge-coupled device) detectors, brightnesses of many astronomical objects can be measured simultaneously with good accuracy. This gives astronomers the ability to survey large areas of the sky repeatedly and automate the process of tracking the brightness of individual stars over time. This brightness is often measured or plotted in physical units (such as ergs per second per unit area), in the magnitude system, or even in relative flux compared to some reference point. These plots (brightness vs. time) are known as *light curves*, and can yield interesting and important information about an astronomical object.

Consider Fig. 1, which shows a fictional example of a light curve for a light bulb. The bulb (perhaps a slow, compact fluorescent) is turned on at t=0 and turned off at t=8. Three distinct patterns can be seen. The most obvious is that, throughout the majority of the time when the light bulb is on, its luminosity appears to remain constant (within observational error for e.g. the human eye). Analysis of this portion of the light curve would seem to confirm normal experience, that light bulbs have a constant brightness while they are on. However, when the switch is first turned on, the light bulb does not go immediately from zero luminosity to its constant value, but instead can be seen to approach it asymptotically. Similarly, when it is turned off, the bulb's luminosity does not drop immediately to zero, but decreases exponentially. By eye, one may notice that it brightens more quickly than it dims, and careful statistical analysis could determine a best fit value for the characteristic time scales of these processes ($^1/_4$ second when turned on and $^1/_2$ second when turned off). In theory, the detailed physical parameters of the object (dimensions, temperature, etc.) could be constrained by this sort of analysis, and one could, without being told originally, identify that this is a light bulb.

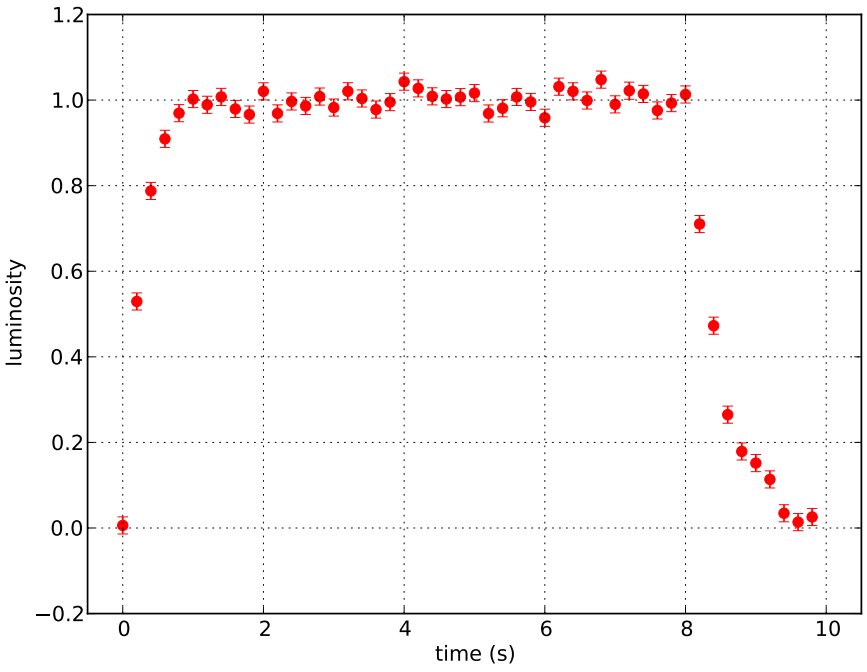

Fig. 1.— A fictional simulation of a light bulb's light curve, in arbitrary luminosity units. The switch is turned on at time 0 and turned off at time 8 seconds. The plot represents luminosity measured 5 times per second with an uncertainty of 0.02 luminosity units. The data was simulated by $L = 1 - e^{-4t}$ for $0 \leq t < 8$ when the bulb is on and $L = e^{-2(t-8)}$ for $8 \leq t < 10$ when the bulb is off. Gaussian random error ($\mu = 0.0, \sigma = 0.02$) was also added to each data point.

From this example of a simple light curve, we can see that what makes a light curve interesting is quite often where it deviates from constant brightness. If analyzed thoughtfully, changes in the brightness of a star can potentially reveal what physical processes are taking place and causing the variation in brightness. A massive increase in the brightness of a star may indicate that the star exploded as a supernova, and the rate at which its luminosity drops can classify the original nature of the star. A star's light curve which shows periodic dips in brightness may indicate it is orbited and periodically eclipsed by another star or even by a planet. If a minor planet spins while it orbits the sun, its light curve may vary periodically as the amount of light it reflects changes regularly. This type of light curve will be of most interest to us in the present work.

1.2. Minor planets and their light curves

Asteroids and other sub-dominant solar system bodies (generally known as *minor planets*) inhabit many different regions of the solar system and are composed of many different materials. Ranging over 5 orders of magnitude in diameter (from Ceres at 952 km, down to tens of meters) some asteroids are little more than orbiting rubble-piles, while the largest are spherical. However, any individual asteroid may have a number of surface discrepancies which can lead to a differential brightness, when viewed from Earth. If an asteroid is non-spherical (as is often the case for the smaller, less massive objects whose internal gravity was not sufficient to form a sphere), then, as it spins, different sides of the asteroid with different cross-sectional areas will face towards the Earth, changing the amount of light reflected. Even for the most spherical asteroids, differences in albedo (how much light is reflected), perhaps due to icy or rough areas across the surface, will lead to variations in brightness as the asteroid spins. Thus, a light curve of an asteroid will most often show a periodic oscillation, from differential reflection or reflective area, in addition to its longer-period trends from orbital motion relative to the Earth and the Sun. From the light curve, this period can be evaluated, and we can discover the spin frequency of many asteroids which are far too small to resolve spatially.

Much is to be gained from accurate information on the spin frequencies of asteroids. Yoshida et al. (2012) highlights the importance of the spin-rate distribution of young asteroid family members (collisional fragments of a disruptional event), as it reflects the original angular momentum distribution of the system before disruption. Detection of tumbling motion (rotation around a non-principal axis) of a non-spherical asteroid, which should be dampened on time scales much less than the age of the solar system due to effects such as stress-strain cycling (Harris 1994), can indicate recent disruption, and increased study of so called "tumblers" can help better understand these damping processes.

In order to effectively disseminate asteroid periods and light curves to those who wish to analyze trends in the many thousands of identified asteroids, Warner et al. (2009) developed the *light curve data base* (LCDB), which today contains published asteroid light curve parameters (such as period and amplitude) as well as physical parameters including size and albedo. Many other

services exist to make this data available and easy to distribute, such as the Minor Planet Bulletin - official publication of the Minor Planets section of the Association of Lunar and Planetary Observers (ALPO), and housed with Warner's LCDB - where most results of minor planet photometric analysis are today published, and the Minor Planet Center's (MPC) own Light Curve Database, which holds complete light curve datasets for theoretical use and modelling of shapes and spin axis. From these large sources of data, interesting features of the asteroid spin distribution have emerged, such as the "spin barrier", where no asteroids above 1 km diameter have found to spin with a period higher than around 2 hours (see Warner et al. 2009).

1.3. Using the HATNet survey for minor planet photometry

The Hungarian-made Automated Telescope Network (*HATNet*; Bakos et al. 2004, 2011; Boisse et al. 2012) survey works to discover extrasolar planets using the transit method.[1] HATNet has been responsible for the discovery of 43 of the ∼200 well-characterized (planetary mass and radius known to 10% accuracy) transiting exoplanets found to date (Boisse et al. 2012). The wide-field survey uses six identical, 11 cm aperture telescopes,[2] four of which are located at the Smithsonian Astrophysical Observatory's Fred Lawrence Whipple Observatory (FLWO) and the other two of which reside on the roof of the Smithsonian Astronomical Observatory's Submillimeter Array at Mauna Kea Observatory (MKO) in Hawaii. Each instrument has (since September 2007) a f/1.8 lens, a 4K × 4K front-illuminated CCD, and a wide 10.6 ° × 10.6 ° field.[3] Operating at a 3.5-minute cadence, one instrument can reach a photometric precision of 4 mmag at the bright end of r ∼ 9.5 (Bakos et al. 2011). Since 2006, HATNet has recorded nearly 1.5 million images, and, thanks to the collaboration of the HATNet team and primary investigator Gáspár Bakos, we are able to utilize these cataloged frames to a secondary use: photometric analysis of asteroids which coincidentally appeared in the images.

In order to maximize the likelihood of identifying the brief, periodic signal of a transiting exoplanet with an orbital period in the range of days to weeks, individual HATs will observe a particular field of the sky (centered on fixed RA/DEC position) continually for extended periods of time. For example, field G205 ($\alpha = 22^h56^m$ $\delta = +37^o30$') was observed every clear night from 2003 September 29 to 2004 February 1, as well as between 2006 July 3 and 2006 July 24 (Latham et al. 2009). Several of the HAT instruments stationed at different longitudes are often scheduled to observe the same fields during a single night, effectively extending the operating time available

[1] Using high-precision photometry to detect an exoplanet eclipsing its host star. See Appendix A for more on the transit method.

[2] Each instrument is known as a HAT

[3] Prior to September 2007, each HAT was outfitted with a 2K × 2K CCD, yielding a field-of-view (FOV) of 8 ° × 8 °. For more on the technical specifications of the HATNet survey, see Bakos et al. 2011.

to observe a single field.[4] G205 was observed by HAT-5 and HAT-6 (FLWO, $\lambda = 111°$W) as well as HAT-8 and HAT-9 (MKO, $\lambda = 155°$W).

With the static, continually observed fields of the HATNet survey and automatically prepared photometric calibration frames such as biases, darks and skyflats (Bakos et al. 2011), one can see that HATNet images could be quite useful for obtaining light curves of minor planets. The wide, $10.6° \times 10.6°$ FOV means that any asteroid which passes through a field is likely to remain in it for a very long time, and could be imaged at a few-minute cadence reliably the entire time. An asteroid with semi-major axis ~ 2.3 AU (inner edge of the Asteroid Belt) will have an orbital period of (from Kepler's 3rd law):

$$\begin{aligned} P &= a^{\frac{3}{2}} \\ &= 3.5\, years \end{aligned}$$

and hence moves at average speed (assuming a circular orbit)

$$\begin{aligned} v &= \frac{2\pi a}{P} && (1) \\ &= \frac{2\pi a}{a^{\frac{3}{2}}} \\ &= 2\pi a^{-\frac{1}{2}} && (2) \\ &= 4.14\, AU\, yr^{-1} \\ &= 1.7 \times 10^6\, km\, day^{-1} \end{aligned}$$

as opposed to $2.58 \times 10^6 \frac{km}{day}$ for the Earth. Thus, at opposition, the Earth moves with velocity $v_E = 8.8 \times 10^5 \frac{km}{day}$ relative to the asteroid. Separated by D = 1.3 AU $= 1.95 \times 10^8\, km$, the apparent angular motion caused by that velocity is:

$$\begin{aligned} \frac{\theta}{day} &\sim \frac{v_E}{D} && (3) \\ &= \frac{8.8 \times 10^5}{1.95 \times 10^8}\, day^{-1} \\ &= 0.0045\, day^{-1} \\ &= 0.26°\, day^{-1} && (4) \end{aligned}$$

An asteroid which moves 0.26° per day (asteroids further away in the Asteroid Belt would have less apparent motion) could thus spend well over a month moving through an individual $10.6° \times 10.6°$ field. While many asteroids may not appear in any yet-studied HATNet fields, and others

[4]An additional benefit of having a network of telescopes at separate locations is to double the chance of having clear observing skies for at least one set of telescopes.

may be too dim to have been recorded (with the 3.5 minute cadence of HATNet images, photometry is most effective for brighter objects), we approached this project with the goal of identifying those bright asteroids which did spend long periods in actively observing HATNet fields. These minor planets could be located in numerous cataloged HATNet images, and, using the already calibrated science frames, we could generate light curves for these objects using only previously cataloged data.

The most important effect for which this project had to account, yet can be mostly neglected in normal HATNet procedures and those of any other fixed object survey, is the significant apparent motion of the minor planets mentioned above. While an asteroid may move 0.26° in a day, it would take Barnard's Star (which has the highest proper motion of any bright star in the sky) nearly 100 years to move the same 0.26°. Thus, while HATNet can treat its targets as fixed in space, we were required to recalculate the position of each asteroid for every frame we wished to analyze. In § 2 we describe this process, including various measures we attempted but discarded, to rapidly and precisely generate positions on the sky for a given minor planet at any point in time. Once a minor planet was located, we transformed its position to a Cartesian, frame-centric coordinate-system in order to evaluate whether it would have been captured by a HATNet frame. This was performed with an ARC projection (Calabretta & Greisen 2002), and this Cartesian system was then converted into a pixel value on the frame. These steps are discussed in § 3. In § 4 of this paper, we highlight the use of HATNet software to perform aperture photometry on the asteroid images and to normalize these measurements against reference stars found in the field. We discuss our findings in § 5, specifically a light curve and rotation period for asteroid 7 (Iris). In § 6, we conclude with a discussion of the difficulties we encountered in generating past ephemerides for minor planets, and offer a suggestion for how an improved system of distributing minor planet orbital elements can encourage the reuse of survey data for minor planet photometry.

2. Minor Planet Ephemerides

In order to analyze the brightness of any object on the sky (whether with a CCD or the naked eye), one must first know where to locate it. To do this for most any star, galaxy, or nebula is quite simple: one can merely look up the right ascension (RA, α) and declination (Dec, δ) of the object from a table or online catalog. These objects are so distant that even incredible relative velocities result in only the slightest of yearly angular displacements.

For objects within our own solar system, however, the position on the sky is far from constant (hence the name "Planet" from the Greek for "wandering star"). The brightest of these planets - Mercury, Venus, Mars, Jupiter, and Saturn - which the ancients noticed and studied, can be seen with the naked eye to cross through constellation after constellation throughout the seasons. The dimmer planets (Uranus and Neptune), while not bright enough to be seen with the naked eye, undergo this same motion, as does every object which orbits the Sun.

To first approximation, the solar system bodies follow Keplerian (i.e. elliptical) orbits, with the Sun at one focus. The semi-major axis (a) determines the scale of the orbit, and the ellipticity (e) sets the shape. While most major bodies orbit in near to the same plane, in general the inclination (i) must also be specified. In total, in order to mathematically describe the position and motion of a solar system body at a particular time (epoch), one must specify six parameters, often 6 spatial parameters or 5 spatial parameters and a time at which the object passed a particular point in its orbit (e.g. time of perihelion).

With these values (known as the *orbital elements*) and Newton's laws of motion, one can determine the position an object on an elliptical orbit around the Sun at any time in the future or past. With similar information on the Earth's orbit, and a defined observation point from the Earth, one can calculate the relative positions of an observer and the solar system object, and hence derive the object's RA and Dec for a given date and time. A collection of these values for given dates and times is known as an *ephemeris* table (or *ephemerides*).

Many services exist to generate ephemerides for astronomers who wish to locate where an object will be in upcoming observations. The Minor Planet Center,[5] (MPC) operating at the Smithsonian Astronomical Observatory, and part of the International Astronomical Union (Spahr et al. 2009), offers browser-based queries for ephemeris tables through their "Minor Planet and Comet Ephemeris Service". This allows the user to generate ephemerides for several hundred objects at a time, and for up to 1440 individual date entries at any specified number of day, hour, minute, or second intervals. While these values are quite accurate and were used in this project to calibrate the accuracy of other ephemeris tables, we were unable to find any interface other than an HTML query form to access these data, and as such entering arbitrary lists of minor planets and non-uniformly spaced times could not be done automatically or reliably.

Other commonly-used options are XEphem,[6] a graphical ephemeris package developed by Elwood Downey for UNIX-type systems, and PyEphem, [7] a package for the Python scripting language, that uses methods from XEphem written in Python and C, to allow the user detailed Python commands to generate ephemerides automatically. In particular, PyEphem allows the input of a minor planet's orbital elements[8], and then calculates the position of that minor planet at any time (and for any particular observer) by evolving the planet's elliptical orbit.

Unfortunately, while PyEphem's ephemeris generator is fast and allows for automated generation of ephemerides at arbitrary times, it relies upon the elliptical description of a planet's orbit. This is a good approximation for the major planets and for short time spans, but in general the

[5]http://www.minorplanetcenter.org/iau/mpc.html

[6]http://www.clearskyinstitute.com/xephem/

[7]http://rhodesmill.org/pyephem/

[8]Our orbital elements were taken from the MPC, which conveniently allows for output of orbital elements in any number of different formats and standards, including XEphem/PyEphem format

orbit of a solar system body is not strictly Keplerian: it is perturbed by the gravity of other bodies in the solar system (primarily Jupiter). To accurately determine the position of an asteroid on the sky, one must take into consideration: 1) the basic Keplerian motion of the Earth, 2) the Keplerian motion of the asteroid, and 3) the perturbations in the asteroid's orbit due to Jupiter and - to a lesser extent - Saturn and the other planets.

To simplify the generation of ephemeris tables for minor planets, the standard practice has become to define an elliptical orbit for the planet, which is valid for a particular range of dates. Orbital elements are published, allowing the position to be calculated to relatively high precision for a limited window (normally, a few weeks to months). During that time, the perturbation effects of Jupiter and the other planets are negligible on top of the elliptical path of the minor planet. As time progresses, however, the perturbations from a Keplerian orbit increase. Near the end of the validity window, a new elliptical orbit is defined, taking into account the recent perturbations, and new orbital elements are distributed. In this manner, any observer who wishes to target a particular solar system body for observation can do so by generating its ephemerides automatically (and throughout the entire observing session) before the observing begins.

The major resources for minor planet information (such as the MPC) publish only these most recent orbital elements, which are most useful to current observing projects. However, because the elements are not valid outside particular ranges, it is impossible to use the currently published orbital elements to calculate ephemerides to arcsecond or even arcminute precision back to 2006 and earlier, as is needed to locate minor planets in our HATNet frames. Thus, to generate the most accurate ephemerides, we relied upon an HTTP request service (Miriade) provided by the Paris Virtual Observatory Data Center.[9] This service calculates highly accurate ephemerides (values computed for randomly selected dates were confirmed to match with those of the MPC) for any particular solar system body, taking perturbation effects into account. It additionally allows command-line queries and the submission of up to 1000 observation epochs simultaneously. Unfortunately, it is significantly slower than the PyEphem calculations, and, with an incredibly high volume of needed ephemeris epochs, it is also not practical to be used exclusively. We concluded that the best approach to identify asteroids which appear within HATNet frames was to combine the use of two different ephemeris services, PyEphem (rapid but imprecise outside a particular date range) and Miriade (time expensive, but highly accurate).

To begin our search, we were given access to a catalog of all science frames taken so far by the HATNet survey. Each entry contained the HAT instrument number, field number, frame identifying number, coordinates (RA and Dec) of the center of the frame, and the date and time when the image was taken. From the date and instrument number, we could determine the FOV of the image (see § 1.3). Over 1.4 million frames were included in the survey, by the time this catalog was developed.

[9] http://vo.imcce.fr/webservices/miriade/

For numbered asteroids - beginning with 1 (Ceres) - we used the MPC orbital elements and PyEphem's ephemeris generator to calculate approximate coordinates for the asteroid at every time listed in the catalog, and compared the calculated position to the frame taken at that time. Because these ephemerides were known to be imprecise, we greatly increased our tolerance for a confirmation: if the position calculated was within one FOV[10] of the frame center, this frame was marked as a potential match, and the asteroid's position at that time was saved.[11]. Both ephemeris generators also yield magnitude estimators, and any frame where an asteroid was predicted to be dimmer than magnitude 15 (the faint end of reliable photometry with HATNet) was not saved. After the majority of frames were excluded from possibly containing the asteroid, we used Miriade to calculate more precise ephemerides for the remaining frames (those in which the asteroid was estimated to be within one FOV). Through combining the two services, we were able to reduce what was originally a several hour run-time per asteroid, when all 1.4 million frames were analyzed by Miriade, to one that took between 90 seconds (for asteroids with few or no potential matches) and 6 minutes (for the asteroids such as 7 (Iris) and 61(Danaë) which had more than 30,000 potential matches each) to calculate all useful ephemerides with no loss of precision.

To motivate our choice to exclude times where the asteroid was more than one FOV away from the center of the frame, despite using an imprecise ephemeris generator, we include in Fig. 2 comparisons of the ephemerides generated by PyEphem and by Miriade. For the points chosen within one FOV of frame center, we calculated the angular distance between the PyEphem, Keplerian approximation and the precise Miriade calculation. While the PyEphem values range by as much as several arcminutes from the correct position, the perturbations do not cause the predicted position to diverge from the correct value. The minor planets can thus be seen to reside on fairly stable orbits around the Sun, and the perturbations caused by the other planets only cause them to oscillate around a Keplerian orbit. As all divergences are well within the several-degree buffer zone we allowed in our selection criteria, we are confident that we did not exclude any instances of asteroids appearing within our frame due to PyEphem's imprecise ephemerides.

3. Locating asteroids in HATNet frames

In order to convert the celestial coordinates of the minor planet into a pixel coordinate on a frame, we first had to covert all RA/Dec celestial coordinates to a Cartesian coordinate system, centered on the frame center, using an ARC or zenithal equidistant projection which is often used as the approximate projection of Schmidt telescopes (Calabretta & Greisen 2002). After points have been projected into this Cartesian system, they can be converted to a pixel value based on

[10]Since the new frames, for example, were $10.6^\circ \times 10.6^\circ$ square, accepting a position within 10.6° of the **center** of the frame doubles its effective FOV.

[11]As the Sun is the dominant force in the asteroid's orbit, it was anticipated that true position on the sky would not differ by more than a few degrees even when perturbed.

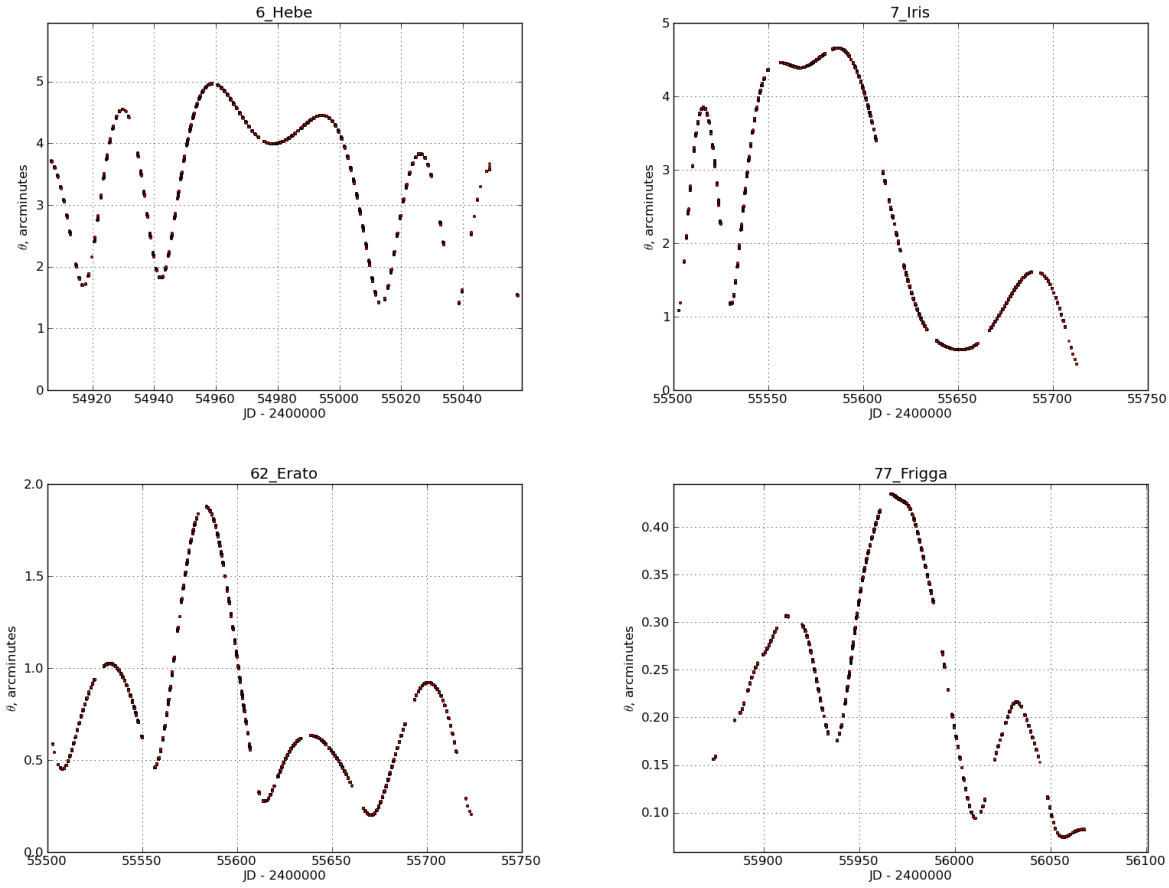

Fig. 2.— Comparisons of Ephemerides generated by PyEphem and Miriade. The ordinate shows the angular separation in arcminutes between the two calculated values for each frame, and the abscissa shows the time the Julian Date the frame was taken. The frames shown are those which were found by PyEphem to be within one FOV from the center of the frame.

the details of the image itself.

3.1. ARC Cartesian projection

The ARC projection shown in Fig. 3 is a way of converting a spherical coordinate system, such as the celestial sphere, onto a flat Cartesian coordinate system. An additional benefit of this projection is that, by projecting the RA and Dec values of the asteroid into a Cartesian system,

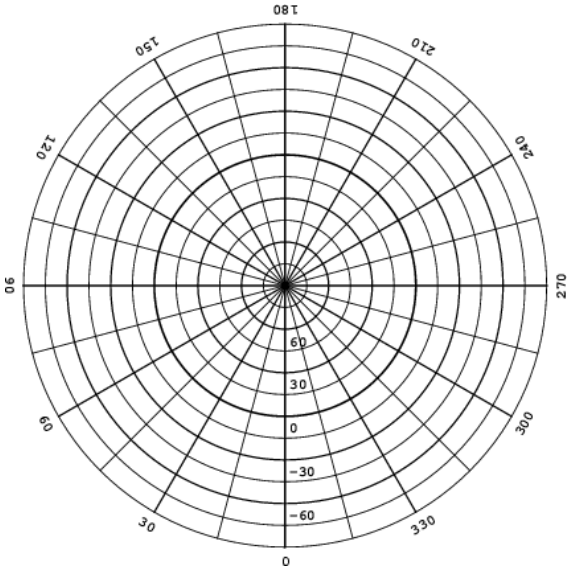

Fig. 3.— The zenithal equidistant (ARC) projection. Image taken from Calabretta & Greisen 2002.

co-centric with the frame, it is trivial to exclude points that do not lie inside the square frame.[12] For each asteroid ephemeris coordinate which was kept as a possible match to lie in a HATNet frame, we converted the α (RA) and δ (Dec) coordinates into Cartesian χ and η (both still in degrees), centered at the frame centric α_0 and δ_0, using the following ARC projection, which was provided by the HATNet team.

$$\chi = \frac{\arccos(A)\,B}{D} \tag{5}$$

$$\eta = \frac{\arccos(A)\,C}{D} \tag{6}$$

where:

$$A = \cos\delta\cos\alpha\cos\delta_0\cos\alpha_0 + \cos\delta\sin\alpha\cos\delta_0\sin\alpha_0 + \sin\delta\cos\delta_0 \tag{7}$$

$$B = -\cos\delta\cos\alpha\sin\alpha_0 + \cos\delta\sin\alpha\cos\alpha_0 \tag{8}$$

$$C = -\cos\delta\cos\alpha\sin\delta_0\sin\alpha_0 - \cos\delta\sin\alpha\sin\delta_0\sin\alpha_0 + \sin\delta\cos\delta_0 \tag{9}$$

$$D = \sqrt{B^2 + C^2} \tag{10}$$

$$\tag{11}$$

Once the asteroid's position was converted to Cartesian coordinates, we removed those which

[12]Projecting the boundary lines of a square onto a sphere and determining if a given point is inside or outside the boundary can be quite difficult.

lay outside of the frame. Since the ARC projection is frame-centric, if $\mid \chi \mid > \frac{1}{2}$FOV or $\mid \eta \mid > \frac{1}{2}$FOV, then the asteroid lay outside that frame when taken. Otherwise, it was determined that the asteroid indeed appeared in the image, and that frame was labeled as a match. After processing for all such frames, we had a list of HATNet frames in which each asteroid should be found, as well as its position coordinates (both in celestial α,δ and in frame-centric χ,η) at the time each frame was taken.

3.2. Calculating FITS frame pixel values

To convert the Cartesian degree values χ and η determined by the ARC projection into a pixel location on a HATNet image required the use of previously developed code from the HATNet team. For each HATNet FITS image, there is a corresponding transformation file, which holds the parameters for a 6th order polynomial astrometric fit between the projected χ,η coordinates of stars in the Two Micron All Sky Survey catalog (Bakos et al. 2011) and pixel location (X,Y). After locating the relevant transformation file for the HATNet frame in question, the original celestial coordinates (α,δ) could finally be converted into a physical location (X,Y) on the FITS frame. After applying this procedure for all matching frames, we generated a file for each asteroid which held a list of the frames in which it appeared, along with the asteroid's coordinates (in all three systems: celestial (α,δ), projected Cartesian (χ,η), and FITS pixel coordinates (X,Y)) at the time the image was taken.

3.3. Selecting 7 (Iris) as a target asteroid

As of this writing, we have executed the preceding steps, from asteroid ephemeris generation to calculating FITS image pixel values, for the first 200 numbered asteroids. However, as the following photometric steps began, we determined that it would only be reasonable to continue with photometry for one individual asteroid at a time. Each step in photometric analysis and calibration was significantly more time expensive than the previous coordinate generation and conversion processes. To maximize our likelihood of receiving a reliable result, we decided to continue the process of photometry on asteroid 7 (*Iris*), due to its high number of matching frames (over 11,000) and its high brightness relative to other asteroids (estimated above magnitude 10 throughout the survey by PyEphem).

4. Photometry

To calculate the brightness of Iris in each FITS frame, we performed fixed-center aperture photometry, centered on the location of the asteroid. The HATNet survey utilizes an effect known as Point-Spread-Function (PSF) Broadening to overcome some of the under-sampling difficulties

involved in wide-field surveys, and this effect is accounted for in the photometry software (Bakos et al. 2004). The brightness of Iris was evaluated by determining the amount of light which was detected by the CCD within a certain radius of the asteroid center (the X,Y pixel value calculated in § 3.2). This is known as aperture photometry, and was performed at three fixed radii, in identical fashion to how the original stellar photometric measurements and calibrations were executed by the HATNet team and continue to be executed in new projects such as the HATSouth survey (Bakos et al. 2012).

After this initial aperture photometry, it was still necessary to cross-calibrate the magnitude calculations to account for effects such as changing extinction and PSF size. This involved calibrating all individual frames in a particular HATNet field against a randomly selected reference frame from that same field. [13] Because a frame from one field cannot be calibrated against another (the reference stars are different), we were required to separate all matching frames into groups by field, and perform photometry separately on the images in each field. However, as discussed earlier, the large FOV of the HATs means that asteroids are likely to spend a long time in any given field. So, while dozens of fields have been mapped over time by the HATNet survey, each asteroid likely appears in only a handful (if any at all). Iris was found in more than 11,000 frames, and yet only appeared in three fields (numbered 317, 365, and 366). Iris' images from field 317 (in which it appeared 5643 times) were selected to continue light curve analysis. Once all field 317 images were processed, and the brightness of Iris measured, the date and time of each frame was converted into a decimal Julian Date (JD). As a result, we knew Iris' brightness as a function of time, and we were able to begin analysis of its light curve.

5. Iris light curve analysis and results

The first procedure required to derive a rotation period for Iris was to model and remove global trends from the light curve data. Fig. 4 shows the initial light curve derived for Iris during the late Autumn to early Winter of 2010. In order to search for periodicities in the data, our first goal was to remove the global trend towards brighter magnitudes over time. We modeled this trend with a fourth order polynomial fit, as a function of JD. Fig. 5 shows this fit, along with the least-squares minimizing parameters, and Fig. 6 shows the residuals from removing this trend from the data.

We used The VARTOOLS Light Curve Analysis Program, developed by Hartman et al. (2008), to analyze periodicities in the Iris magnitude residuals. We performe an AoV phased binning period search (Schwarzenberg-Czerny 1989; Devor 2005). Phase-folding of the data around the primary period of 0.4463 ± 0.0008 days (10.71 ± 0.019 hours) generated with this method did not produce a clearly periodic result. Also using VARTOOLS, we removed this primary harmonic

[13] As part of this adjustment, we also applied a first-order color fit to account for extinction. This required an estimated color value for each asteroid, which we assumed to be the same as the Sun (J-H = 0.3).

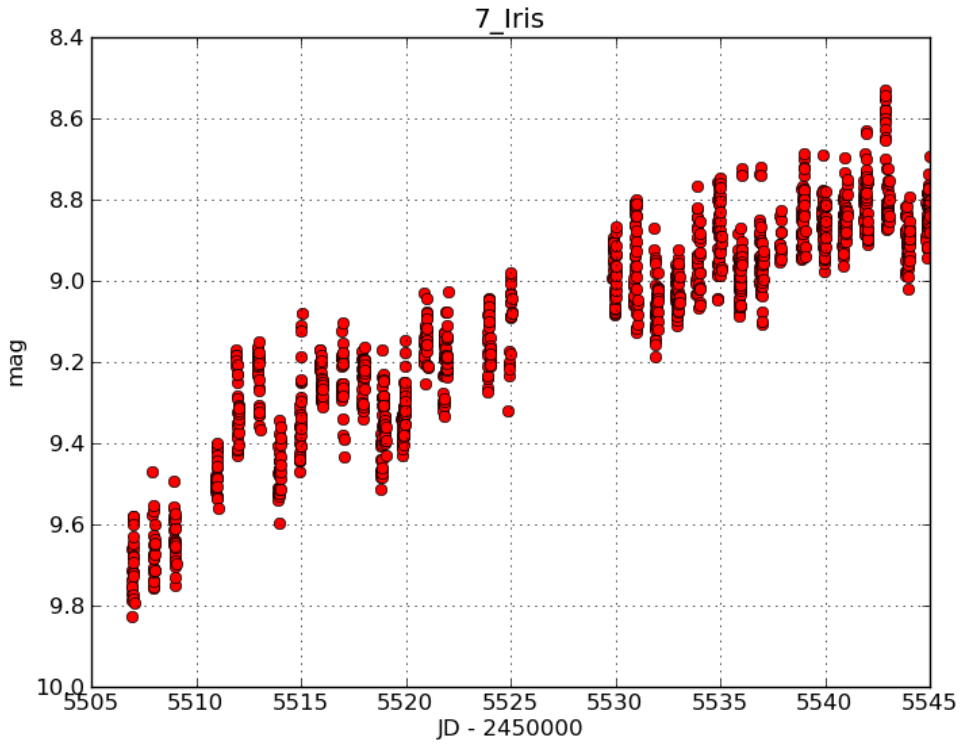

Fig. 4.— The original light curve for asteroid 7 (Iris), as determined from photometry performed on HATNet images. Images included in this light curve were taken between 2010 November 4 and 2010 December 14 by HAT5, located at FLWO. Large variations of brightness within a given night can be seen, as well as a global night-to-night trend towards brighter magnitudes, due to Iris approaching opposition with Earth (the MPC confirms that closest approach between the two came on 2011 January 15).

with a whitening, and the next period generated by the AoV period search was 0.2975 ± 0.0005 days (7.141 ± 0.012 hours).[14] Fig. 7 shows the Iris light curve data phase-folded about this period (red points) and a weighted-sum binning of the same (black diamonds). This period matches very closely the results of literature (see Table 1). Additionally, it can be seen that the original primary harmonic period found using AoV is very nearly 1.5 times this calculated period, so the false period generated was likely a statistical artifact. However, there is still quite noticeable vertical variation around the phased average sinusoid. One explanation for this variation could be a changing light curve shape which, although keeping the same periodicity, will lead to increased scatter in a phased composite light curve taken from many different dates.

[14]Uncertainties in the period were evaluated as one half of the full width at half maximum of the period's peak in the AoV power spectrum.

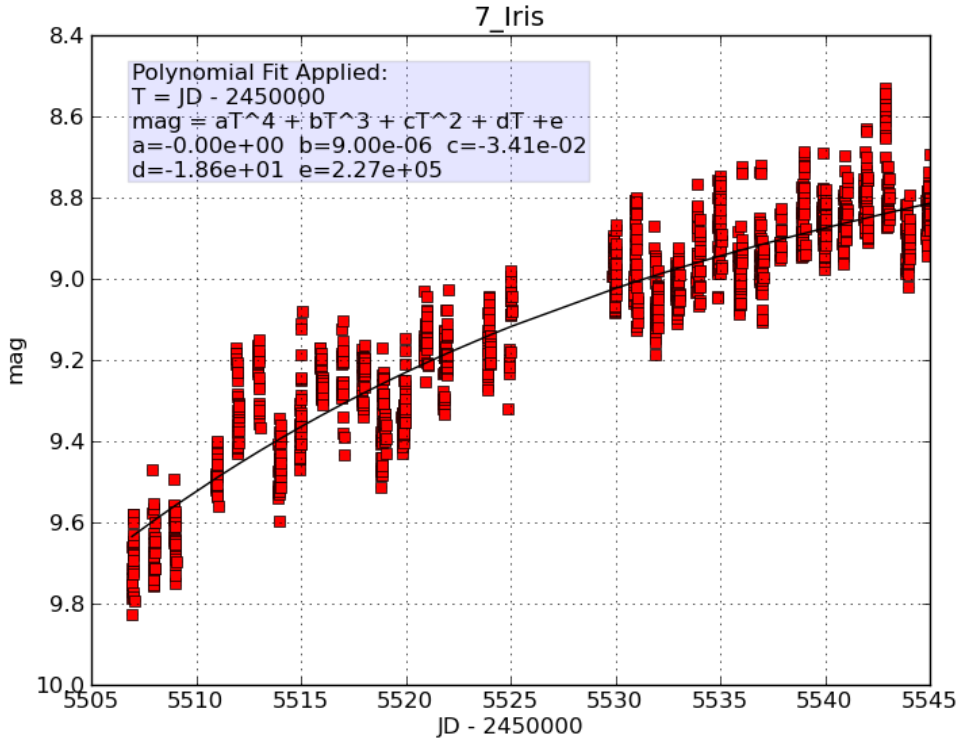

Fig. 5.— The Iris light curve with a fourth order polynomial fit to magnitude as a function of JD.

Of particular interest in the light curve of Iris (both in this work and the literature) is the presence of two well defined peaks and their relative intensities. The homogeneity of Iris' surface is a highly disputed issue, and while the asteroid seems to be mineralogically homogeneous, there is mounting evidence to support the proposition that Iris has large, irregular regions across its surface (Ostro et al. 2010). While Hollis (2001) finds no deviations in their light curves and infer from this that the surface is sufficiently homogeneous as to be undetectable to a visual observer, Hoffmann & Geyer (1993) notes that previous light curves indicate the two maxima to be variable and of different brightnesses. They conclude that Iris is likely covered in a fine distribution of spots and regions of generally different albedo, and could even have a large bright region in its northern hemisphere.

The images from which our light curve was generated were taken during a 40 day period when Iris was approaching opposition with Earth (suggested by the night-to-night increase in brightness and confirmed by the MPC). This changing perspective, combined with the strong tilt of Iris' rotation axis with respect to its orbital plane (Hoffmann & Geyer 1993) and its possible surface variations could result in long-period variations in the shape and relative heights of Iris' maxima, leading to the observed spread in the phased light curve. This could be to blame for the relatively

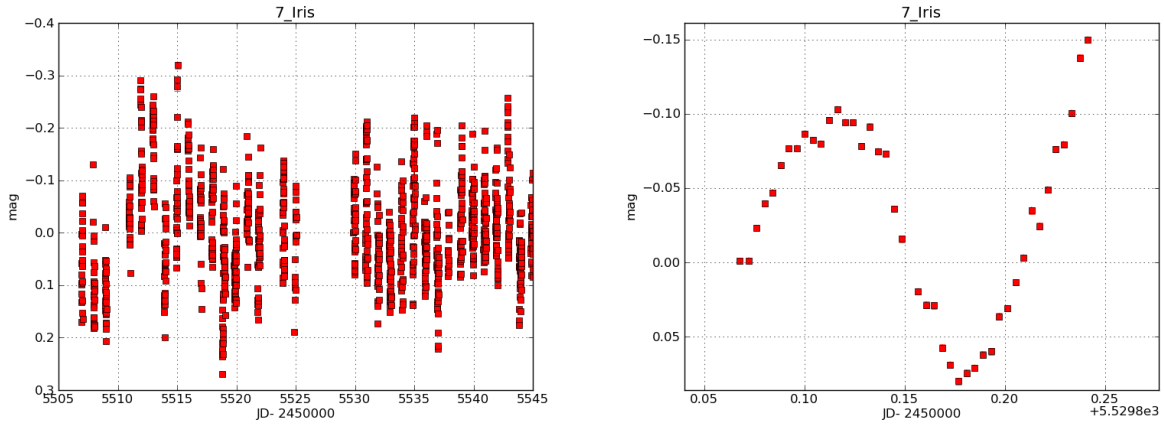

Fig. 6.— The left panel shows the residuals between the polynomial fit and the light curve data. The right panel shows the same residuals, but zoomed in on the data gathered on 2010, Nov. 29. While night-to-night scatter still exists after the fit, the light curves of individual nights are still strongly sinusoidal.

7 (Iris)		
Reference	Period (h)	Error (h)
Hollis (2001)	7.137	0.005
Kaasalainen et al. (2002)	7.138841	0.000005[15]
Ostro et al. (2010)	7.1388	0.0001
Ďurech et al. (2011)	7.138840	0.000005
This work	7.141	0.012

Table 1: References to a selection of published rotation periods for 7 (Iris). Resources were gathered from the LCDB (Warner et al. 2009).

high (compared to the literature) uncertainty in the rotation period of Iris. With a better trend filtering procedure which accounts for the changes in the relative amplitude of the maxima, we believe that the large magnitude scatter, and thus the uncertainty in the period, could be greatly reduced.

6. Discussion

As mentioned in § 1.3, this work's most unique addition to the HATNet survey's capacity is the introduction of a method by which minor planets can be located and identified within previously imaged HATNet frames. Unlike most any other target which HATNet or similar surveys study, a minor planet cannot be treated as having a fixed position for more than a few minutes. However, once minor planets are located, HATNet has the immense benefits of well calibrated photometric

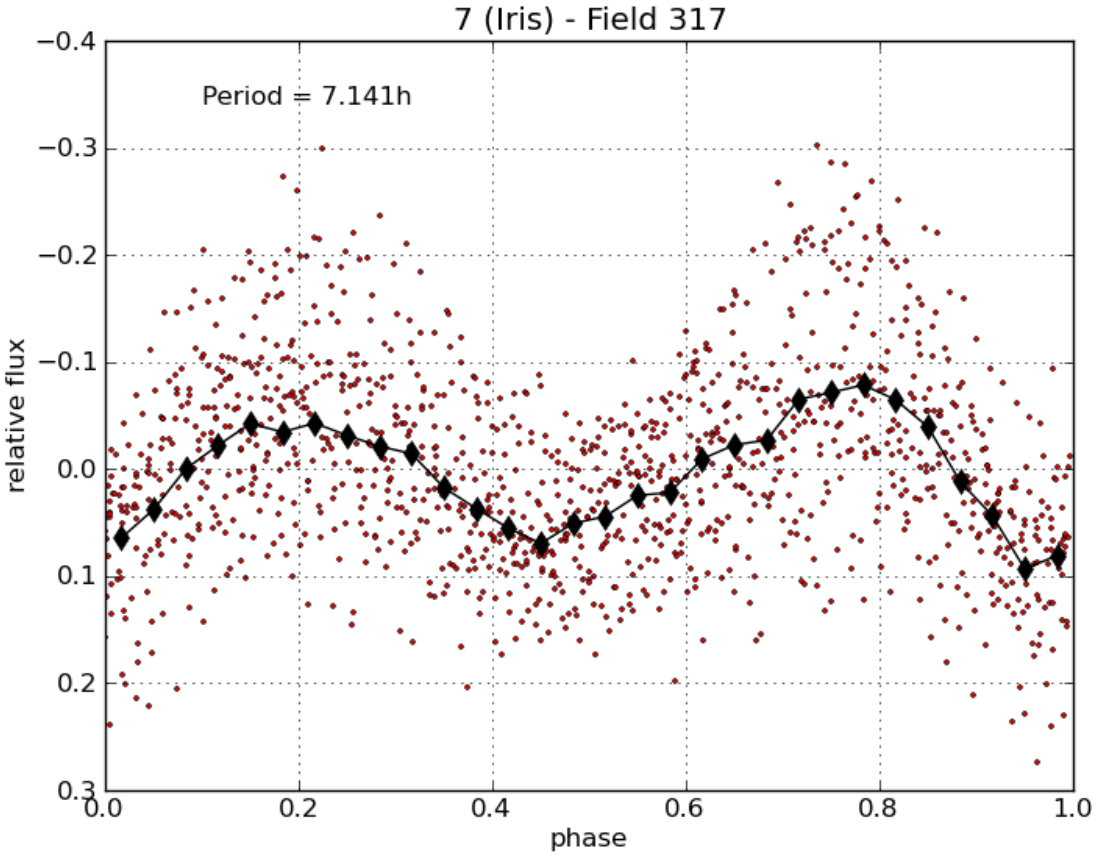

Fig. 7.— Phase-folded light curve of 7 (Iris). Red dots represent phase-folded data, while black diamonds are a weighted average binning of the same. The period of phase is 7.141 hours.

references, wide FOVs, and long periods of frequent study for any particular field.

One of the largest roadblocks to using recycled data for minor planet photometry is the difficulty of generating past ephemerides in an automated, accurate, and rapid way. Many of the most reliable minor planet resources (such as the MPC) focus on enabling observers to generate ephemerides for short periods in the future. The standard which has evolved of publishing only temporary Keplerian elements that rapidly become obsolete is of little practical use for those who wish to reverse engineer past ephemerides.

What we suggest would help encourage the reuse of survey and other observational data to study minor planets would be simply an easy-to-access database, available through the Minor Planet Center or elsewhere, of published orbital elements, *past and present*. If a single line of ASCII text is enough to predict the position of an asteroid to arcsecond accuracy within a month's time frame, then a file with a few dozen lines of previously published orbital elements for a minor planet could

enable programs such as PyEphem to retain complete precision for years into the past. By reusing frames designed for other purposes, generating minor planet light curves is cheap and effective, and an astronomer can add to the growing field of minor planet research without needing to compete for equipment or observing time.

The author wishes to acknowledge and thank Professor Gáspár Bakos for his advice and constant support throughout this project, and for kindly providing access to the HATNet data and software. He also thanks Zoltan Csubry for his help in navigating files and software, Joel Hartman for providing the VARTOOLS code to analyze light curves, and the rest of the HATNet team for their discussion and advice. It has been a pleasure working with all of you.

This research has made use of IMCCE's Miriade VO tool.

This paper represents my own work in accordance with University regulations.

REFERENCES

Bakos, G., Noyes, R. W., Kovács, G., Stanek, K. Z., Sasselov, D. D., & Domsa, I. 2004, PASP, 116, 266

Bakos, G. Á., Csubry, Z., Penev, K., Bayliss, D., Jordán, A., Afonso, C., Hartman, J. D., Henning, T., Kovács, G., Noyes, R. W., Béky, B., Suc, V., Csák, B., Rabus, M., Lázár, J., Papp, I., Sári, P., Conroy, P., Zhou, G., Sackett, P. D., Schmidt, B., Mancini, L., Sasselov, D. D., & Ueltzhoeffer, K. 2012, ArXiv e-prints

Bakos, G. Á., Hartman, J. D., Torres, G., Kovács, G., Noyes, R. W., Latham, D. W., Sasselov, D. D., & Béky, B. 2011, in European Physical Journal Web of Conferences, Vol. 11, European Physical Journal Web of Conferences, 1002

Boisse, I., Hartman, J., Bakos, G., Penev, K., Csubry, Z., Beky, B., Latham, D., Bieryla, A., Torres, G., Kovacs, G., Buchhave, L., Hansen, T., Everett, M., Esquerdo, G., Szklenar, T., Falco, E., Shporer, A., Fulton, B., Noyes, R., Stefanik, R., Lazar, J., Papp, I., & Sari, P. 2012, ArXiv e-prints

Calabretta, M. R. & Greisen, E. W. 2002, A&A, 395, 1077

Devor, J. 2005, ApJ, 628, 411

Harris, A. W. 1994, Icarus, 107, 209

Hartman, J. D., Gaudi, B. S., Holman, M. J., McLeod, B. A., Stanek, K. Z., Barranco, J. A., Pinsonneault, M. H., & Kalirai, J. S. 2008, ApJ, 675, 1254

Hoffmann, M. & Geyer, E. H. 1993, A&AS, 101, 621

Hollis, A. J. 2001, Journal of the British Astronomical Association, 111, 26

Kaasalainen, M., Torppa, J., & Piironen, J. 2002, Icarus, 159, 369

Latham, D. W., Bakos, G. Á., Torres, G., Stefanik, R. P., Noyes, R. W., Kovács, G., Pál, A., Marcy, G. W., Fischer, D. A., Butler, R. P., Sipőcz, B., Sasselov, D. D., Esquerdo, G. A., Vogt, S. S., Hartman, J. D., Kovács, G., Lázár, J., Papp, I., & Sári, P. 2009, ApJ, 704, 1107

Ostro, S. J., Magri, C., Benner, L. A. M., Giorgini, J. D., Nolan, M. C., Hine, A. A., Busch, M. W., & Margot, J. L. 2010, Icarus, 207, 285

Schwarzenberg-Czerny, A. 1989, MNRAS, 241, 153

Spahr, T. B., Williams, G. V., & Marsden, B. G. 2009, Transactions of the International Astronomical Union, Series A, 27, 183

Ďurech, J., Kaasalainen, M., Herald, D., Dunham, D., Timerson, B., Hanuš, J., Frappa, E., Talbot, J., Hayamizu, T., Warner, B. D., Pilcher, F., & Galád, A. 2011, Icarus, 214, 652

Warner, B. D., Harris, A. W., & Pravec, P. 2009, Icarus, 202, 134

Winn, J. N. Exoplanet Transits and Occultations, ed. S. Seager, 55–77

Yoshida, F., Ito, T., Dermawan, B., Nakamura, T., Takahashi, S., Ibrahimov, M. A., Malhotra, R., Huen Ip, W., Chen, W. P., Sawabe, Y., Haji, M., Saito, R., Hirai, M., Miyasaka, S., Fukushima, H., Sato, H., & Sato, Y. 2012, ArXiv e-prints

A. The transit method of exoplanet detection

If a star is orbited by a planet whose orbital plane is oriented randomly in the sky, there is a chance that the planet will eclipse its star when viewed from Earth (this is known as a transit). The signal of the transit can be detected by accurately monitoring the brightness of the host star. When the planet passes in front of the star, a small piece of the star's cross-sectional area will be covered, and thus the star will appear to emit less light. For a star-planet pair such as the Sun and Earth ($R_\oplus \sim .01 R_\odot$), the planet would cover $^1/_{10{,}000}$ the area of the star, and the star's brightness would decrease by approximately 1 part in 10,000. For a star-planet pair similar to the Sun and Jupiter ($R_J \sim .1 R_\odot$), this effect would be closer to 1 part in 100, and is identifiable with modern CCD detectors. Additional details extracted from the shape of the host star light curve, combined with follow-up radial velocity measurements, can yield estimates of the planetary mass and radius with better than 10% precision.[16]

This preprint was prepared with the AAS LaTeX macros v5.2.

[16]For a technical introduction into exoplanet transits, see Winn 2011.